Hydrogenic impurity states in quantum-well wires: Shape effects

Garnett W. Bryant
McDonnell Douglas Research Laboratories, P.O. Box 516, St. Louis, Missouri 63166
(Received 4 March 1985)

The binding energies for the bound states of a hydrogenic impurity placed in a quantum-well wire are calculated with the use of variational solutions to the effective-mass equation. The quantum-well wire is a quasi-one-dimensional region of GaAs. The electrons are confined to this region by an infinite barrier. The calculations are performed to determine the effect that the shape of the wire's cross section has on the binding energies. Results for quantum-well wires with rectangular cross section are determined and compared with results previously obtained for cylindrical quantum-well wires. The results for cylindrical wires with diameter w and for square wires with width w are nearly identical. Even closer agreement occurs between the results obtained for cylindrical and square wires with equal cross-sectional area. When the wire becomes nonsquare by expanding one side while keeping the other side fixed, the binding energies drop rapidly to the values appropriate for two-dimensional wells of finite thickness. When the wire becomes nonsquare by expanding one side and contracting the other side to maintain a constant cross-sectional area, the binding energies change very slowly. The binding energies approach the values expected for narrow two-dimensional wells only after the cross section has deviated substantially from being square. The results indicate that the binding energies for impurities in wires with comparable shapes are most closely correlated to the cross-sectional area.

I. INTRODUCTION

Understanding the impurity states in semiconductor microstructures is an important problem in semiconductor physics. The impurity levels and exciton states in quasi-two-dimensional quantum wells and superlattices have been well calculated.[1–14] Two calculations[15,16] have also been performed for the hydrogenic impurity levels of a quantum-well wire (QWW). The studies for two-dimensional wells and for wires are complementary. In the former, the electron motion is free in the two dimensions of the well but is quantized in the direction perpendicular to the well. In the QWW, electron motion along the wire axis is free but is quantized in the two dimensions perpendicular to the wire axis.

Quantum-size effects become increasingly important as the well width or the dimensions of the wire's cross section become small. The effect of the Coulomb interaction is enhanced by the electron confinement. For hydrogenic impurities in quasi-two-dimensional wells which are modeled using an infinite barrier for the confining potential, the binding energy of the lowest bound state approaches $4R_e$, where R_e is the effective rydberg,[17] as the well width decreases. The enhancement of the binding energy is even greater in QWW's due to the additional electron confinement. The binding energy of a hydrogenic impurity on the wire axis approaches infinity as the radius of a cylindrical QWW decreases[15,16] if the confining potential is an infinite barrier. For a realistic wire with a finite barrier,[15] the confining potential becomes ineffective when the wire is very small and the binding energy approaches the value for an impurity in the material surrounding the wire. Although the binding energies never are infinite in realistic QWW's, the binding energies are still two or three times greater than the values in comparable quasi-two-dimensional wells. For a QWW made from a cylinder of GaAs surrounded by $Ga_{1-x}Al_xAs$, the effect of the Coulomb interaction is enhanced when the wire dimensions are much below 0.1 μm. The confinement becomes ineffective when the wire dimensions are less than 5 nm, and qualitative differences between the results obtained with the infinite barrier and realistic models become significant.

One effect not addressed by any of the calculations mentioned is the effect that the shape of the microstructure has on the binding energy. This issue is not raised for two-dimensional wells because they do not have shape. It is a moot point for structures with large dimensions since the confinement of the impurity potential will keep the bound electron away from the boundary. Nevertheless, the electron wave function must conform to the shape of the boundary near the edge of a QWW. When the dimension of the QWW is comparable to the size of the bound state (the effective Bohr radius in GaAs is 10.3 nm), the effect of shape should be considered.

This paper explores the effect that the shape of the QWW has on impurity binding energies when the QWW is in the quantum-size regime. This is done by determining the impurity states for QWW with rectangular cross sections and comparing these results with results obtained previously for wires with circular cross section.[15]

A simple estimate can be made for the shape effects in realistic wires with finite confining barriers. The effect of a change in cross section can be included in first-order perturbation theory if the old and new cross sections are similar and the barrier is finite. When the electron motion perpendicular to the wire axis can be described using a single level, the same first-order energy shifts due to the change in shape are predicted for the electron bound

to the impurity in the new QWW and for the free state of the new QWW without impurities. Thus there should be no net effect of shape on the binding energy any time that first-order perturbation theory is adequate and the motion perpendicular to the axis is well quantized to one level. The radial motion of the lowest impurity bound state in a circular QWW is well quantized to a single level for a wide range of wire sizes (the one-subband approximation gives binding energies with less than 10% error for wires with diameters from 2.5 nm to >50 nm). Our study of shape effects will help determine how dissimilar the shapes must be before first-order perturbation theory becomes inadequate and the shape effects become significant.

Intuition suggests that binding energies for on-axis impurities in wires with different cross sections should be similar when some geometric parameter for each wire is similar. Three possible parameters that could be correlated with the binding energy are the minimum dimension, the maximum dimension, and the area of the wire's cross section. We will determine the parameter which is most closely correlated to the binding energy.

The calculations reported in this paper were performed using the infinite-barrier model for the confining potential. There are several reasons for using the infinite-barrier model. The results for cylindrical QWW's indicate there are no qualitative differences for the impurity binding energies of realistic and infinite-barrier QWW's unless the wire diameter is less than 5 nm. Thus the shape effects for realistic and infinite-barrier QWW's are expected to be qualitatively similar except for the smallest wires. Moreover, shape changes cannot be treated as small perturbations for infinite-barrier wires so that shape effects should be more dramatic for infinite-barrier wires.

The practical reason for using the infinite-barrier model is that the calculations are much easier to perform in this case. The calculations proceed by using the free solutions of the QWW without an impurity to define the basis functions for the bound-state wave function. The effective-mass Schrödinger equation for an impurity in the QWW is solved to determine the eigenenergy. By using the basis functions for the free levels, the effects of the confining potential are automatically included and only a limited basis set is needed to obtain accurate binding energies. Basis functions which describe the quantized motion in the well perpendicular to the wire axis are easy to define analytically for infinite-barrier cylindrical wires, for realistic cylindrical wires, and for infinite-barrier rectangular wires. For a realistic rectangular wire, motion in the two directions which define the rectangular well is not separable, making an analytic definition of the basis functions very difficult. In fact the author is unaware of any analytic determination of the free solutions of a realistic rectangular well. It is beyond the scope of the present calculations to make a numerical determination of the basis functions prior to beginning the intended calculations of the binding energies.

In Sec. II the model for the rectangular QWW and the method used to determine the eigenstates are outlined. The results are presented in Sec. III, and the implications for shape effects are discussed in Sec. IV.

II. THEORY

The same model and method of solution are used for rectangular wires as were used in Ref. 15 for cylindrical wires. In the present calculations, the wire's cross section is a rectangular well, defined by an infinite barrier. The well region is GaAs with conduction-band effective mass $m_e=0.067m_0$, where m_0 is the free mass, and dielectric screening $\epsilon=13.1$. The effective rydberg R_e in GaAs is 5.3 meV. The results presented in Sec. III are scaled by this value. The donor impurity is modeled as a point-charge impurity. The charge can be located anywhere in the well. Dielectric screening of the point charge is included by scaling the impurity potential by the static dielectric constant ϵ.

The electron bound states are found by solving the effective-mass Schrödinger equation. Normally, the effective mass equation is reliable only for weakly bound states. One might worry that the effective mass approach becomes inappropriate when the binding energy is greatly enhanced in QWW's. However, the band gap of GaAs (1.4 eV) is 300 times R_e so that effective mass approximation is adequate for our purposes.

The Schrödinger equation to be solved is

$$\frac{-\hbar^2}{2m_e}\nabla^2\Psi-\frac{e^2}{\epsilon|\mathbf{r}-\mathbf{r}_i|}\Psi=E\Psi, \quad |x|\le w_x/2,\ |y|\le w_y/2 \tag{1}$$

where x and y are the directions which define the rectangular well and w_x and w_y are the well widths. The boundary condition imposed on Ψ requires that Ψ vanish on the boundary of the rectangular well. The impurity is located at $\mathbf{r}_i$.

Equation (1) is solved by expanding Ψ in terms of products of basis functions of x, y, and z (the direction parallel to the wire axis),

$$\Psi(\mathbf{r})=\sum_{i,j,k}C_{ijk}X_i(x)Y_j(y)Z_k(z)\ . \tag{2}$$

The basis sets $\{X_i\}$ and $\{Y_j\}$ are chosen to be the solutions for the one-dimensional infinite wells defined by the rectangular well. For example,

$$X_n(x)=\left[\frac{2}{w_x}\right]^{1/2}\cos(k_nx),\ \text{for } n \text{ odd}\ , \tag{3a}$$

and

$$X_n(x)=\left[\frac{2}{w_x}\right]^{1/2}\sin(k_nx),\ \text{for } n \text{ even}\ , \tag{3b}$$

where $k_n=n\pi/w_x$ and the energy is

$$E_n=\hbar^2k_n^2/2m_e\ .$$

Similar functions are used for the Y_j.

The z basis functions Z_k are chosen to be Gaussian,

$$Z_k(z)=N_k\exp(-\tfrac{1}{2}\xi_kz^2)\ , \tag{4}$$

where N_k is the normalization constant. Only even-parity solutions are considered, and the impurity is located at $z_i=0$. A reliable set of ξ_k was determined[15] by solving

the one-dimensional Coulomb problem using this basis set. The binding energy could be predicted with less than 0.1% error using the set $(\xi_k a_e^2)=(0.17,0.47,1.4,5.6,39.0)$ where $a_e=\epsilon(m_0/m_e)a_0$ is a scale factor, the effective Bohr radius, which accounts for the dielectric response and effective mass of the material and a_0 is the Bohr radius. For GaAs, $a_e=196a_0=10.3$ nm. For eigenstates with low binding energy, the basis set was augmented to include $\xi_k a_e^2=0.02$ and 0.1, which provide more extended basis functions. This basis set was sufficient for the previous calculations done for cylindrical QWW's.

The Hamiltonian matrix $\langle ijk \mid H \mid stv \rangle$ and the overlap matrix $\langle ijk \mid stv \rangle$, where $\langle xyz \mid ijk \rangle = X_i(x)Y_j(y)Z_k(z)$, are determined using the basis functions. Since $\{Z_k\}$ is not an orthogonal set, the overlap matrix has off-diagonal elements and the generalized eigenvalue problem must be solved for the energy E:

$$\sum_{s,t,v} (\langle ijk \mid H \mid stv \rangle - E\langle ijk \mid stv \rangle)C_{stv}=0 . \tag{5}$$

The energies are minimized by increasing the number of X_i and Y_j used. Little additional minimization was obtained previously[15] by varying the ξ_k, so they were kept fixed. Eigenstates with different symmetries are investigated by using only basis functions with those symmetries. The binding energy is found by taking the difference between E and the appropriate subband energy when no impurity is present.

The only matrix elements in Eq. (5) which cannot be calculated analytically are the matrix elements of the impurity potential. To evaluate these matrix elements, the following representation of the Coulomb potential is used,

$$\begin{aligned}\frac{1}{|\mathbf{r}-\mathbf{r}_i|} &= \frac{1}{\sqrt{\pi}}\int_0^\infty dt\, t^{-1/2}\exp(-t\,|\mathbf{r}-\mathbf{r}_i|^2) \\ &= \frac{1}{\sqrt{\pi}}\int_0^\infty dt\, t^{-1/2}\exp[-t(x-x_i)^2] \\ &\quad \times\exp[-t(y-y_i)^2]\exp[-t(z-z_i)^2].\end{aligned} \tag{6}$$

With this representation, the x, y, and z integrals which determine the impurity-potential matrix element can be done independently and analytically. The results for the x and y integrals are combinations of complex error functions of t, while the z integral is a power of a rational polynomial of t. The matrix element is then determined by doing the t integration numerically. This is the only integral which must be done numerically.

III. RESULTS

All solutions can be classified by their parity in the z direction, along the wire axis, relative to the impurity. In this paper only states with even z parity are considered. The enhancement of the binding energy by the confinement is much less for states with odd z parity than for even z-parity states. Our results for cylindrical QWW's show that the radial spread of states with odd z parity is no greater than the radial spread for similar states which have even z parity. These two facts suggest that the shape effects should be smaller for odd z-parity states.

When the impurity is located on the wire axis, the solutions can also be classified by their parity in the x and y directions relative to the wire axis. The ground state of an on-axis impurity is even (with the wave function defined using cosine basis states) in both the x and the y directions. This state corresponds to the $1s$ state in the three-dimensional limit. Higher-s states are also determined using states with even x and y parities. For these states the z basis states must have nodes. Since our basis set does not contain such states, higher-s states are not determined.

The excited states considered here are those which have even parity in one direction perpendicular to the axis and odd parity (with the wave function defined using the sine basis states) for the other direction perpendicular to the wire axis. The lowest states with this symmetry correspond to the $2p_x$ and $2p_y$ states in the three-dimensional limit. When the $x(y)$ parity is odd the solution is a $2p_{x\,(y)}$ state. Solutions with odd parity in both the x and y directions can also be considered. Since they were not considered previously,[15] they are not discussed in detail here.

Figures 1 and 2 show results for the lowest bound state ($1s$) when the impurity is on the wire axis. In Fig. 1 the binding energies E_B for square wires of width w are com-

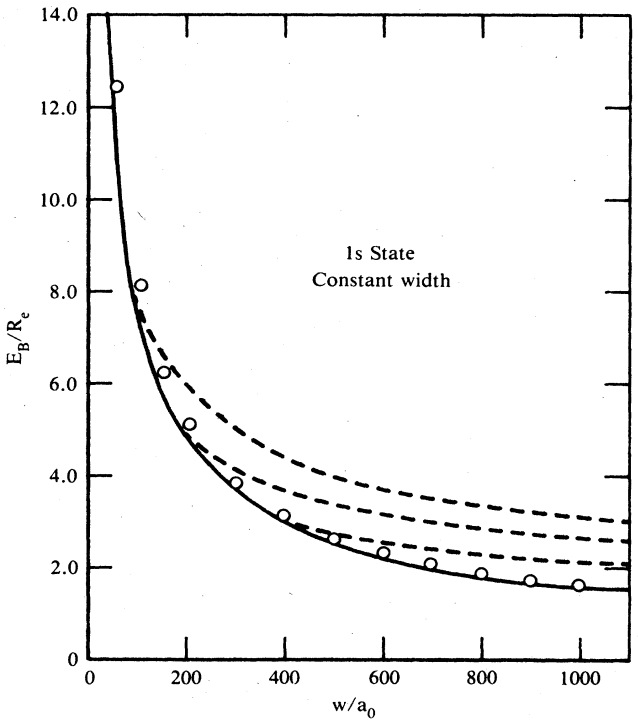

FIG. 1. Binding energy E_B for the ground state ($1s$) of a hydrogenic impurity on the axis of a quantum-well wire. The solid curve is for square wires with width w. The open circles are for cylindrical wires of diameter w. The dashed curves are for rectangular QWW's which have one dimension fixed at the values of w where the dashed curves intersect the solid curve and the other dimension given by w. Results for wires with fixed widths of $100a_0$, $200a_0$, and $400a_0$ are shown. The binding energy is scaled by the effective rydberg R_e (in GaAs, $R_e=5.3$ meV) and the width by the atomic Bohr length a_0.

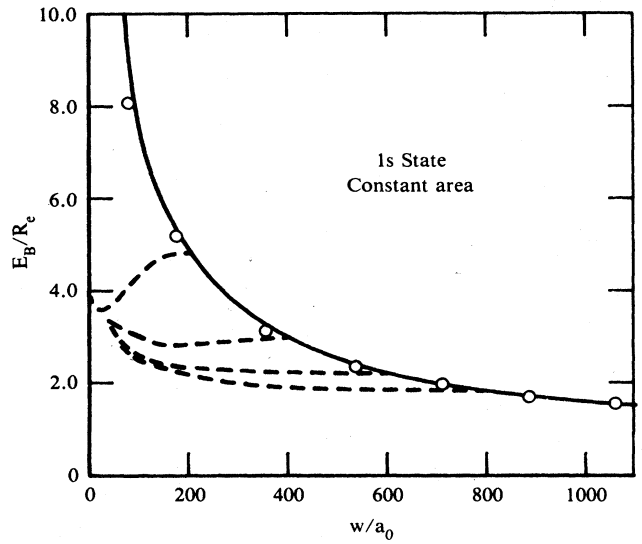

FIG. 2. Binding energy E_B for the ground state ($1s$) of a hydrogenic impurity on the axis of a QWW. The solid curve is for square wires with width w. The open circles are for cylindrical wires with cross-sectional area w^2. Each dashed curve is for rectangular wires with constant cross-sectional area, which is the same as for the square wire at the point where the curves intersect. The dimension of the short side of the rectangle is given by w.

pared with the E_B for cylindrical QWW's with diameter w. The results for the cylindrical QWW's are slightly higher because the cylindrical QWW's provide greater confinement than do square QWW's with the same dimension. The shape effects are small. The E_B differ by slightly less than 5% for $w \approx 1000a_0$ and by about 6% for small w ($w \approx 100a_0$).

Although the shape effects are small when the E_B of square and cylindrical QWW's are compared, the effects are more significant when the wire has unequal sides, as indicated by the rapid decrease in E_B that occurs when the wire expands in one direction while remaining fixed in the other direction (see the dashed curves in Fig. 1). For small expansions of one side, the wave function expands in that direction to conform to the new wire geometry. After sufficient expansion of the side the confinement due to the impurity potential becomes more important than the confinement due to the well and E_B approaches the value expected for an impurity at the center of a two-dimensional well with finite thickness. We did not attempt to reach this limit using our basis states (cosine solutions) for the expanding direction since too many basis states would be needed in this limit to get accurate results. It should be noted that the changes shown in Fig. 1 are typical of the changes expected for experiments in which the electrons in a two-dimensional well are confined to a quasi-one-dimensional channel using an applied field.[18]

When the wire contracts in one dimension while remaining fixed in the other direction, the additional confinement enhances the binding. The magnitude of the increase in E_B is similar to the magnitude of the decrease when one side expands. For a $200a_0 \times 200a_0$ wire, for example, E_B decreases by $1.1R_e$ when one side doubles in length and increases by the same amount when one side is reduced by one-half.

Figure 2 compares the results for square QWW's with those for cylindrical QWW's with the same area. The differences are less than 5% for small wires and are visually unobservable for larger wires. The binding energy in the square QWW's is higher because there is more confinement for certain directions in the square QWW's than in cylindrical QWW's with the same area. The binding energies are more closely correlated to the cross-sectional area than to a specific dimension of the cross section. This is especially true when the sides of the well are unequal. The dashed curves in Fig. 2 show E_B for rectangular QWW's with constant cross-sectional area. There is little change in E_B for rectangular QWW's of constant area and nearly equal sides. For large wires the dimensions can change by 30—50%, provided that the area is fixed, without changing E_B. This insensitivity to shape results from the delicate balance between the compensating changes in E_B due to the simultaneous contraction and expansion of the different dimensions. For smaller wires, which are more sensitive to boundary effects, significant changes in E_B occur after smaller changes in the dimensions.

Two different types of changes in E_B occur in Fig. 2 when the sides of the QWW become unequal. If the wire is large, then E_B increases monotonically as the sides become more unequal and approaches the two-dimensional limit $4R_e$ for a hydrogenic impurity in a very narrow well. This behavior indicates that the enhancement of E_B due to the additional confinement in the contracting dimension dominates the effect of the expansion in the other direction when the wires are large. When the wires are small, the effect of the expansion dominates when the sides initially become unequal and E_B decreases. This decrease continues until the wire is so large in the expanding dimension that the boundary has little influence on the bound state. Then the effect of the extra confinement takes over and E_B increases to the two-dimensional limit.

The extent of the insensitivity of E_B to the shapes of QWW's with equal area is surprising considering that the wave function must conform to the shape of the boundary near the edge of an infinite-barrier well. One cannot argue that confinement effects are small because the enhancement of E_B is substantial for all QWW shapes and dimensions considered. However other factors make the E_B for cylindrical and square QWW's of equal area so similar. When the areas are equal, only 9% of the area of the circle is not contained in the overlap with the square. There is little area for the electron to occupy which is not common to both. Moreover, the deviations from circular symmetry in the wave function for the lowest eigenstate of the square well are small until the wave function is small. For example, the contour of points where the wave function is one-half its value on the wire axis is only 3% noncircular. Also, the eigenvalues for the free levels in square and circular wells are similar. When the wells have equal area, the eigenvalue of the lowest level in the square well is 8% higher than that in a circular well, in-

dependent of the well size. Moreover, the lowest energy level changes by less than 10% when the dimension of a rectangular well changes by 20% provided the area is constant. E_B is less sensitive to the shape of the wire because the confinement of the impurity keeps the bound electron away from the boundary.

Figure 3 shows how the binding energy of the $1s$ state changes when the impurity is moved off the wire axis. For illustration, a square QWW of dimensions $200a_0 \times 200a_0$ is considered. The solid curve shows the decrease in E_B as the impurity moves from the origin to the center of a side along the line $y=0$. The dashed curve shows the decrease as the impurity moves out along the diagonal $x=y$. The difference in the two curves is due almost entirely to the way the dashed curve is plotted. When the dashed curve is replotted as a function of the distance between the impurity and the wire axis, the new curve (the circles) lies almost on the solid curve. This close agreement is indicative of the strong quantization of the electron to the center of the wire even when the impurty is off the wire axis. When the wire is larger, the quantization should not be as complete and the results should not lie so close together.

When the impurity is located at symmetry points on the boundary, the bound states and binding energies are identical to other bound states and binding energies for impurities at the center of larger wires. For example, the $1s$ level of an impurity at a corner must be identical to the $3d_{xy}$ state of an impurity on the axis of a wire which is twice as large in each direction. The $1s$ level of an impurity at the center of one of the edges $x=\pm w_x/2$ must be identical to the $2p_x$ level of an impurity on the axis of a QWW which is twice as large in the x direction. The results satisfy these identities, indicating that the motion in the wells has been properly incorporated.

The binding energies for states with odd parity in one direction perpendicular to the wire axis, the $2p_x$ and $2p_y$ states, are shown for wires of constant width in Fig. 4 and constant area in Fig. 5 as in Figs. 1 and 2. For square QWW's, the $2p_x$ and $2p_y$ states are degenerate and a single solid curve is shown in each figure. The results for square and circular QWW's with the same width or same area are very close. In fact, the agreement is closer for the $2p_x$ and $2p_y$ states than for the $1s$ states. One might expect the boundary to affect odd-parity states more since they are pushed out toward the boundary. However, the energy separation between the two lowest odd states is greater than the energy separation between the two lowest even states. Thus there is less mixing of higher odd states into the solution and less sensitivity to the boundary.

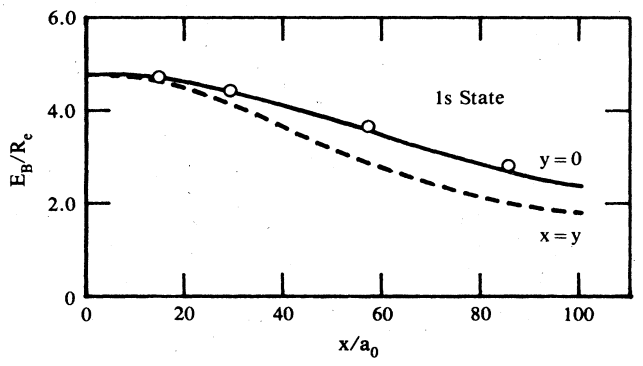

FIG. 3. Binding energy of the lowest bound state ($1s$) of an impurity off the QWW axis. The wire has a square cross section of $200a_0 \times 200a_0$. Denoting the coordinates of the impurity by x and y with the wire axis at the origin, the solid curve is for $y=0$ and the dashed curve for $x=y$. The open circles shown are results taken from the dashed curve for $x=y$ and replotted as a function of the distance of the impurity from the origin.

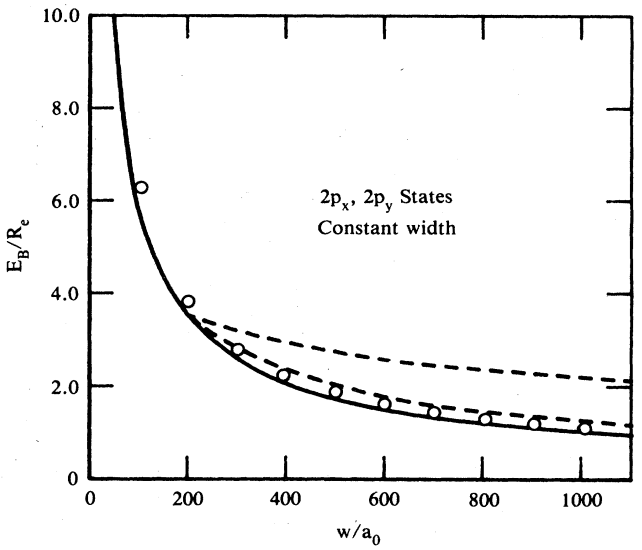

FIG. 4. The binding energy E_B of the $2p_x$ and $2p_y$ excited states of an impurity on the axis of a QWW. The solid curve is for wires with square cross section (width w) and the open circles are for cylindrical wires with diameter w. The dashed curves are for rectangular QWW's with constant width ($200a_0$) in one direction and width w in the other direction. For the upper curve the p lobe points perpendicular to the expanding side, and for the lower curve the p lobe is parallel to the expanding side.

When the boundary has unequal sides, the binding energy does depend on the shape and the degeneracy between the $2p_x$ and $2p_y$ states is lifted. The state with the p lobe pointing parallel to the long side of the rectangle has the lower binding energy. This result is understood by the following argument. The $2p_x$ and $2p_y$ states are degenerate when the cross section is square. As one side expands, the states become less confined by the barrier in that direction. After sufficiently large expansion, the bound states are determined in the expanding direction by the confinement due to the impurity potential, independent of the boundary. In that limit the $2p$ state with odd parity in the expanded dimension has lower binding energy. To reach this lower limiting value, the binding energy for the $2p$ state with the lobe pointed parallel to the expanding dimension must decrease faster. In Fig. 5, the p lobe is parallel to the long (short) side of the QWW in the lower (upper) dashed curve. Thus the two E_B in Fig. 5 approach different two-dimensional limits.

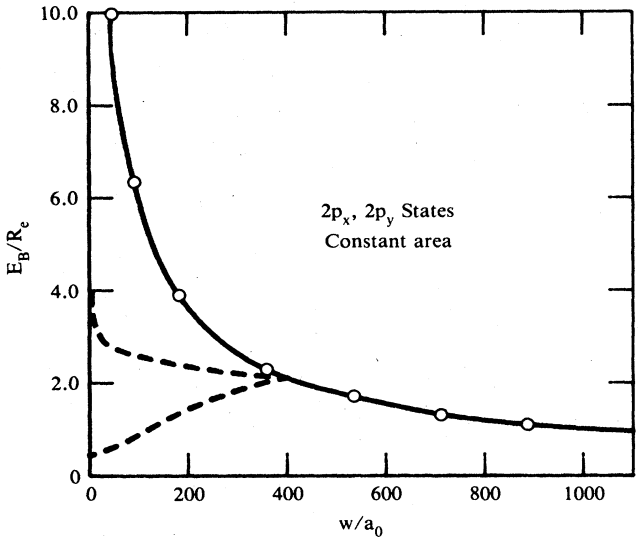

FIG. 5. The binding energy E_B of the $2p_x$ and $2p_y$ excited states of an impurity on the axis of a QWW. The solid curve is for wires with square cross section (width w) and the open circles are for cylindrical wires with area w^2. The dashed curves are for rectangular QWW's with constant area and are plotted as in Fig. 2. For the upper curve, the p lobe points perpendicular to the expanding side, and for the lower curve the p lobe points parallel to the expanding side.

The E_B were determined by including enough subbands for each well direction to obtain accurate results. The number of basis states needed to describe motion in one direction was determined by the width of the well in that direction and was insensitive to the other well dimension. Only the lowest basis state had to be included when the well was less than $200a_0$ wide. The E_B changed by 1% when a second basis state was included for a $200a_0$ well. For a $600a_0$ well, the E_B changed by about 4% when a second basis state was used, but only by 1% when a third was added. For $1000a_0$ wells, three states were used. For wells wider than $1000a_0$, the results were sometimes qualitatively, as well as quantitatively, incorrect when only the lowest subband was used in the solution.

IV. CONCLUSIONS

The binding energies for the $1s$, $2p_x$, and $2p_y$ bound states of a hydrogenic impurity placed in a quantum-well wire have been calculated by finding solutions to the effective-mass equation. Results for quantum-well wires with rectangular cross section were determined and compared with results previously obtained for cylindrical QWW's to determine the effect that the shape of the wire has on the binding energies.

The results for wires with square cross section and for cylindrical wires are qualitatively the same if the dimensions of the wires are comparable. In fact, the results are nearly identical if the cross-sectional areas are equal. If the binding energies were independent of the wire shape, then the binding energies would be correlated with some geometrical parameter describing the wires, such as the minimum dimension, the maximum dimension, or the cross-sectional area. The results show that the binding energies are most closely correlated to the cross-sectional area. Binding energies increase when one of the dimensions of the rectangle contracts and the binding energies decrease when one dimension expands. These changes in binding energy are comparable for comparable changes in dimension. For a wide range of wire dimensions, this delicate balance insures that the binding energy depends on the cross-sectional area and not on the actual shape.

The shape effects in realistic QWW's with finite barriers will vanish whenever first-order perturbation theory accurately describes the shape effects and the one-subband approximation accurately describes the quantized motion. The results for infinite-barrier wires show that the one-subband approximation is adequate, with errors in the binding energy of less than 10% for wells with dimensions less than $1000a_0$. Even so, the shape effects are still pronounced and substantial changes in E_B do occur for substantial changes in QWW shape. Thus, shape effects should occur in realistic QWW's when the shapes are so different that first-order perturbation theory fails. The shape effects in realistic QWW's may be smaller but they should be qualitatively similar to the effects reported in this paper.

ACKNOWLEDGMENTS

This work was performed under the McDonnell Douglas Independent Research and Development program.

[1]C. Mailhiot, Y.-C. Chang, and T. C. McGill, Phys. Rev. B **26**, 4449 (1982).
[2]R. L. Greene and K. K. Bajaj, Solid State Commun. **45**, 825 (1983).
[3]G. Bastard, Phys. Rev. B **24**, 4714 (1981).
[4]G. Bastard, E. E. Mendez, L. L. Chang, and L. Esaki, Solid State Commun. **45**, 367 (1983).
[5]G. Bastard, E. E. Mendez, L. L. Chang, and L. Esaki, Phys. Rev. B **26**, 1974 (1982).
[6]R. L. Greene and K. K. Bajaj, Solid State Commun. **45**, 831 (1983).
[7]R. C. Miller, D. A. Kleinman, W. T. Tsang, and A. C. Gossard, Phys. Rev. B **24**, 1134 (1981).
[8]D. A. Kleinman, Phys. Rev. B **28**, 871 (1983).
[9]W. T. Masselink, Y.-C. Chang, and H. Morkoç, Phys. Rev. B **28**, 7373 (1983).
[10]R. L. Greene, K. K. Bajaj, and D. E. Phelps, Phys. Rev. B **29**, 1807 (1984).
[11]S. Chaudhuri and K. K. Bajaj, Phys. Rev. B **29**, 1803 (1984).
[12]S. Chaudhuri, Phys. Rev. B **28**, 4480 (1983).
[13]F. Crowne, T. L. Reinecke, and B. V. Shanabrook, Solid State Commun. **50**, 875 (1984).

[14]C. Priester, G. Allan, and M. Lannoo, Phys. Rev. B **29**, 3408 (1984).
[15]G. W. Bryant, Phys. Rev. B **29**, 6632 (1984).
[16]J. Lee and H. N. Spector, J. Vac. Sci. Technol. B **2**, 16 (1984).
[17]The effective rydberg is $R_e = Rm_e/\epsilon^2$ where $R = 1$ Ry, m_e is the electron effective mass (in units of the electron mass), and ϵ is the static dielectric constant.
[18]A. B. Fowler, A. Hartstein, and R. A. Webb, Phys. Rev. Lett. **48**, 196 (1982).